ELSEVIER

Biochimica et Biophysica Acta 1185 (1994) 213–220

BBA Biochimica et Biophysica Acta

Microenvironments of tyrosine D^+ and tyrosine Z^+ in Photosystem II studied by proton matrix ENDOR

Hiroyuki Mino, Asako Kawamori *

Faculty of Science, Kwansei Gakuin University, Uegahara 1-1-155, Nishinomiya 662, Japan

(Received 3 December 1993)

Abstract

Proton matrix ENDOR spectra of tyrosines $Z^+(Y_Z^+)$ and $D^+(Y_D^+)$ were studied in the frozen Tris-treated PS II. ENDOR spectra of the tyrosines in oriented membranes observed at 10 K have shown similar angular dependence with similar line pair separations, suggesting that the local arrangement of protons surrounding both radical species is similar. The angular dependence of EPR spectra showed the C-O bonds in Y_Z^+ and Y_D^+ lie parallel to the membrane normal. With increasing temperature, the intensity of the line pair with 1.2 MHz separation decreased above 25 K for Y_Z^+, and above 110 K for Y_D^+, respectively. Assuming a motion of the proton responsible to the line pair, the activation energies for the motional broadening were estimated to be 86 ± 20 J/mol for Y_Z^+, and 810 ± 200 J/mol for Y_D^+, respectively. The broadening may be ascribed to small amplitude vibrations of protons surrounding tyrosine radicals. The intensities for the peaks with about 7 MHz separation assigned to the OH proton of the tyrosine decreased, which was ascribed to a similar motional broadening. The difference in temperature dependence of line broadening of the two radicals suggests that the functional difference between them may be ascribable to differences in flexibility in their microenvironment.

Key words: Tyrosine D^+; Tyrosine Z^+; Tris-Photosystem II; Photosystem II; EPR; ENDOR; Motional broadening

1. Introduction

Two tyrosine residues have recently been identified as redox active components of the PS II electron transport chain [1–4]. One of them, Y-161 of the D1 polypeptide, is called Z, the component that reduces the oxidized reaction center chlorophyll, $P680^+$, and transfers the oxidizing equivalent to the oxygen-evolving complex [1,2]. The other, Y-161 of the D2 polypeptide, corresponds to the component D on the donor side of PS II that has a stable radical state Y_D^+ [3,4]. Tyrosine D functions as a donor to one of the S states of OEC or as an acceptor to Q_A^-, depending on its redox state [5,6]. The proteins, D1 and D2, construct the structural C_2 symmetry around the reaction center chlorophyll P680. However, the electron transfer functions are different between these proteins. The oxidized Y_D^+ has a remarkable stability at room temperature; its EPR signal is known as signal II_s [7]. On the other hand, the oxidized Y_Z^+ in the oxygen evolving PS II has a very short lifetime and its EPR spectrum, referred to as signal II_{vf}, can be observed only with difficulty [8]. These differences might be ascribed to the local structure of D1 and D2 proteins in the PS II. The elimination of OEC by washing with a Tris buffer results in the increase of the lifetime of Y_Z^+ [9], so that the EPR signal, referred to as $Sig.II_f$, can be observed more easily. Furthermore, the formation of oxidized Y_Z^+ in a low pH buffer or in Tris-treated PS II was slowed as monitored by optical absorption changes [10]. From the temperature dependence of the rate of Y_Z oxidation, the activation energies were estimated to be 45 kJ [11] in Tris-washed PS II and 10 kJ in the S_1 state of the oxygen-evolving PS II [12]. The differences in the oxidation rate and the activation energy were explained by structural changes around Y_Z [12] or by a

* Corresponding author. Fax: +81 798 510914.

Abbreviations: PS II, Photosystem II; OEC, the oxygen-evolving complex; Y_D, a tyrosine electron donor in the D2 subunit of PS II; Y_Z, a tyrosine electron donor in the D1 subunit of PS II; signal II_s, EPR signal of Y_D^+; signal II_f, EPR signal of Y_Z^+; Mops, 4-morpholinopropanesulfonic acid; ENDOR, Electron Nuclear Double Resonance; ESEEM, Electron Spin Echo Envelope Modulation.

SSDI 0005-2728(94)00006-Q

charge effect of the membrane surface [13]. Each tyrosine molecule is linked with an amino acid of surrounding proteins through a hydrogen-bonded proton. The estimated activation energies suggest displacement of the OH proton from the tyrosine molecule. The rocking movement of the proton was suggested to contribute to the electron transfer functions of both tyrosine molecules [12,14].

Both EPR signals, signal II_s and signal II_f, show the same hyperfine splitting with the intensity ratio about 1:3:3:1, which can be ascribed to couplings with one of the β-methylene protons and two equivalent 3,5-ring protons [15]. A slight difference [16] has recently been found in lineshapes between signal II_s and signal II_f, which has been ascribed to the difference in the dihedral angle of the β-methylene proton [17]. Using ESEEM spectroscopy, Evelo et al. determined the hydrogen-bonded proton coupling constants $A_{iso} = \pm 1.6$ MHz and $T_{11} = \pm 8.4$ MHz [18].

In order to account for the unusual stability of Y_D^+ compared to Y_Z^+ the microenvironments of both radicals should be studied. Svensson et al. have elaborated a molecular model of Photosystem II based on analysis of the protein sequences and computer simulations, and suggested that the environment of Y_D^+ is more hydrophobic than that of Y_Z^+ [19].

Proton matrix ENDOR spectra provide structural information based on the magnetic dipole interaction between the electron spin and surrounding protons, such as those from the immediate protein environment [20,21]. The intensity of the ENDOR signal is influenced by line width and spin lattice relaxation, both of which depend on the dynamical properties of the molecules. We have previously shown preliminary results on the differences in motional properties between Y_D^+ and Y_Z^+ in Tris-treated PS II by ENDOR spectra within the frequency range of 3 MHz [22]. We were able to trap Y_Z^+ at a high efficiency of 90% at 253 K, because the rate of reduction Y_Z^+ was slowed down by freezing of the membrane lipid. Naturally, it would be desirable to trap Y_Z^+ in the untreated PS II to observe the microenvironment of Y_Z^+. To date, no such attempt has been successful. The temperature dependence of the intensities of the manganese multiline and $g = 4.1$ signals showed that Y_Z oxidation might occur even at 80 K in the oxygen-evolving PS II [23], in which case Y_Z^+ could not be trapped.

In this paper, we study the difference between Y_D^+ and Y_Z^+ in more detail and with greater accuracy by proton matrix ENDOR to get an insight into the relevance of the microenvironment and the electron transfer mechanism in PS II. Investigation of the temperature dependence of ENDOR spectra will give information on dynamical properties of the microenvironment of the both radical species, as well as their structural properties at low temperatures.

2. Materials and methods

Oxygen-evolving PS II membranes (300–500 μM O_2 (mg Chl)$^{-1}$ per h) were prepared from market spinach by the method of Kuwabara and Murata [24]. The membranes were suspended in 0.8 M Tris buffer (pH 8.5) and stirred under room light for 30 min at 0°C. After centrifugation of the suspension at $35000 \times g$, the pellet was washed with a buffer (0.4 sucrose/20 mM NaCl/20 mM Mops/NaOH (pH 6.8)) three times. Samples in calibrated quartz tubes were prepared to a final pellet of concentration about 15 mg Chl/ml. For the measurement of orientation dependence, PS II membranes were dried on pieces of mylar sheets at 4°C for 12–16 h using nitrogen gas under controlled humidity [25]. Six 2.5×25 mm^2 dried mylar sheets were put into an EPR tube. The samples were illuminated with a 500 W tungsten-Br_2 lamp for 30 s at 253 K and subsequently frozen within 1 s in liquid nitrogen resulting in trapping of 80–90% of Y_Z^+. After dark adaptation for 30 min at 0°C, only the Y_D^+ radical remains, as proved by the kinetics of decrease in EPR intensity at the field position of $g = 2.0117$.

The ENDOR spectra were recorded on a Varian E-109 EPR spectrometer equipped with a ENDOR system made in our laboratory [26]. Experiments above 90 K were performed using a home-made continuous nitrogen gas flow cryostat. An ESR-900 Oxford Instruments continuous flow cryostat was used for experiments below 90 K. A paramagnetic crystal of $CaCu(CH_3COO)_4 6H_2O$ in a fine quartz capillary was inserted into a sample tube to monitor the temperature using the Curie-law behavior of the EPR intensity. After the measurement of the illuminated sample, it was dark adapted for 30 min at 0°C. To calibrate the intensities of EPR signals for the change in the cavity Q-value on replacing samples, the Cr^{3+} in MgO was attached inside the cavity. The signal of the dark adapted sample was subtracted from that of the illuminated one to obtain accurately the signal of Y_Z^+ alone. Though the obtained ENDOR signal for Y_Z^+ showed a lower S/N ratio compared to that for Y_D^+, reproducible signals could be obtained in each experiment.

3. Results

Fig. 1a shows the EPR spectra of overlapped signal II_s and signal II_f after illumination for 30 s at 253 K. After dark adaptation at 273 K for 30 min, only signal II_s of Y_D^+ remains as shown in Fig. 1b. Subtraction of the spectrum in Fig. 1b from that in Fig. 1a gives the spectrum of the signal II_f of Y_Z^+ shown in Fig. 1c. Fig. 1b and Fig. 1c are similar in their line shape. However, a slightly larger separation is seen in the hyperfine splitting due to the central two peaks and the overall

linewidth is correspondingly broader in Fig. 1c, as seen in [16]. A slight overlapping of the Chl^+ radical [27] is observed at the center of the spectrum in Y_Z^+ (Fig. 1a and c) and its intensity depends on sample preparation conditions. ENDOR signals were observed in the PS II membranes with negligible intensity of Chl^+ radical signal.

Fig. 2a and b show the ENDOR spectra of Y_D^+ and Y_Z^+, respectively, within 3 MHz frequency range. The ENDOR spectra for Y_D^+ have been analyzed in detail based on dipolar interactions and ascribed to the matrix protons with distances of between 3.5 and 6.7 Å from the center of tyrosine molecule [28]. We have noticed that both radicals gave almost the same ENDOR spectra below 10 K, which suggests that the configurations of matrix protons in Y_Z^+ and Y_D^+ are similar. However, slight differences exist between the two spectra.

In a point dipole approximation, which gives a good fit with experiments in this frequency range [28], the separation $\Delta\nu$ between ENDOR lines, and the proton-electron distance r are related as follows;

$$\Delta\nu = g\beta g_n\beta_n(1 - 3\cos^2\theta)/r^3 \quad (1)$$

where g and β are the electronic g-factor and Bohr magneton, respectively. g_n and b_n are the nuclear g-factor and magneton. θ is the angle between the r-vector and the magnetic field direction. Thus the same proton can give rise to a set of strong peaks with the splitting $A_\perp$ corresponding to $\theta = 90°$ and an extra set of weak peaks with splitting $A_\parallel = 2A_\perp$ corresponding to $\theta = 0°$ in the first derivative of powder ENDOR spectra. These multiple sets of peaks are said to be coupled, although the peak pairs for $A_\parallel$ are not always observed.

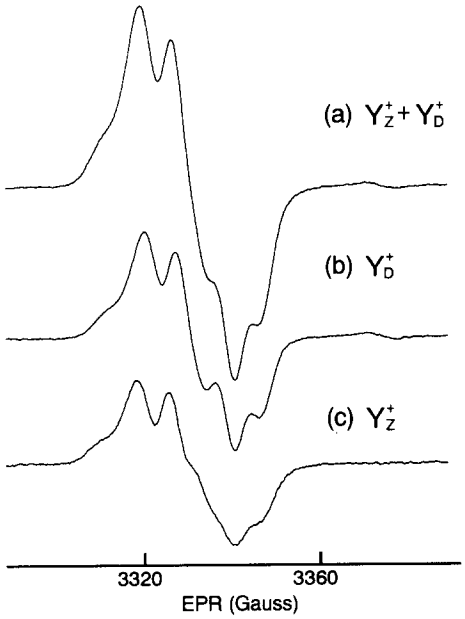

Fig. 1. (a) Overlapped EPR spectra of Y_D^+ and Y_Z^+. Y_Z^+ was trapped at 77 K immediately after illumination at 253 K. (b) EPR spectrum of signal II_s after dark adaptation of the same sample at 273 K for 30 min after observation of (a). (c) EPR spectrum of Y_Z^+ obtained by subtraction (a)–(b). EPR conditions: Microwave frequency, 9.25 GHz; microwave power, 0.05 mW; field modulation frequency, 100 kHz; modulation amplitude, 5 G; temperature, 77 K.

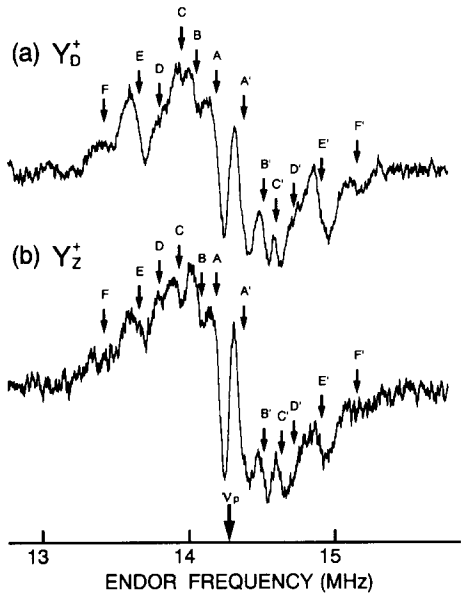

Fig. 2. ENDOR spectra of Y_D^+(a) and Y_Z^+(b) within the frequency range of 3 MHz. The magnetic field was fixed at the center of the EPR spectrum. ENDOR spectrum of Y_Z^+ was obtained by subtracting the spectrum of the dark adapted sample from that of the illuminated sample, as in Fig. 1. ENDOR conditions: Microwave frequency, 9.39 GHz; microwave power, 0.5 mW; frequency modulation (FM), 10 kHz; FM depth, 30 kHz; temperature, 10 K.

In the spectrum of Y_D^+ (Fig. 2a), the shoulder DD′ peaks ($A_\parallel$ component) are coupled with BB′ peaks ($A_\perp$). The EE′ peaks overlap with these $A_\parallel$ components of CC′ peaks ($A_\perp$) [28]. For Y_Z^+ (Fig. 2b) the CC′ peaks have a little larger separation compared to those in Y_D^+. The smaller intensity of the EE′ in Y_Z^+ can be attributed to a slight shift in the position of the $A_\parallel$ components of the CC′ peaks ($A_\perp$). This shift and a little larger width of the lines lower the resolution of the Y_Z^+ ENDOR spectrum. The ENDOR separations obtained from Fig. 2 for all the $A_\perp$ lines are listed in Table 1. The separations for Y_D^+ gave similar values,

Table 1
ENDOR peak separations (MHz) assigned for Y_D^+ and for Y_Z^+ within 3 MHz observed at 10 K

Peak	AA′	BB′	CC′	EE′	FF′
Y_D^+	0.16	0.48	0.66	1.23	1.69
Y_Z^+	0.16	0.43	0.71	1.21	1.67

The absolute error is estimated to be about 0.05 MHz, while the error in relative frequency separations is estimated to be less than 10 kHz.

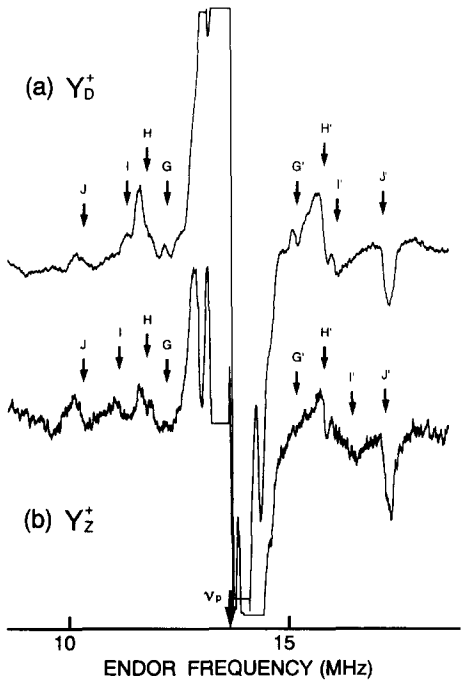

Fig. 3. ENDOR spectra of Y_D^+ (a) and Y_Z^+ (b) in the range of 10 MHz. The spectrum of Y_Z^+ was obtained by subtraction of (a) from the spectrum of the illuminated sample as in Fig. 2. ENDOR conditions: Microwave power, 2 mW; FM modulation, 10 kHz; FM depth, 120 kHz; temperature, 20 K.

within experimental error, as those observed in oxygen-evolving PS II [28] obtained at 100 K.

Figs. 3a and 3b show the matrix ENDOR spectra of both of Y_D^+ and Y_Z^+ recorded at 20 K over a broader frequency range. Though the point dipole approximation is not directly applicable to the widely delocalized

Table 2
ENDOR peak separations (MHz) in the Y_D^+ and Y_Z^+ in the broader frequency range at 20 K

Peak	GG′	HH′	II′	JJ′
Y_D^+	2.94	4.11	4.68	6.80
Y_Z^+	2.91	4.08	5.26	6.90

The errors are same as in Table 1.

electronic spin over a molecule of 3 Å in size and the contact hyperfine interaction is significant for these ENDOR spectra, we may suggest the difference in the position of protons from the difference in the ENDOR separations qualitatively. The II′ peaks in the spectra of Y_Z^+ (Fig. 3b) have a larger separation than that found for Y_D^+ (Fig. 3a). Therefore the II′ proton is considered to be closer to Y_Z^+ than that to Y_D^+. The ENDOR separations from Fig. 3 are given in Table 2.

Fig. 4 shows the EPR spectra of (a) Y_Z^+ and (b) Y_D^+ in oriented membranes. The anisotropy in the EPR spectra can be assigned mainly to that in hyperfine splitting of 3,5-ring protons, since the hyperfine splitting observed between the two central peaks of the β-methylene proton is almost isotropic. Both radical species have a maximum peak separation at the field direction normal to the membranes, and the minimum peak separation at the direction perpendicular to the membranes. It was shown in [28] that the C-O bond of the Y_D^+ radical is parallel to the membrane normal. The anisotropy in the hyperfine separation for 3,5-ring protons shows the same tendency in both radical species, suggesting that the C-O bond for Y_Z^+ is also aligned approximately parallel to the membrane normal.

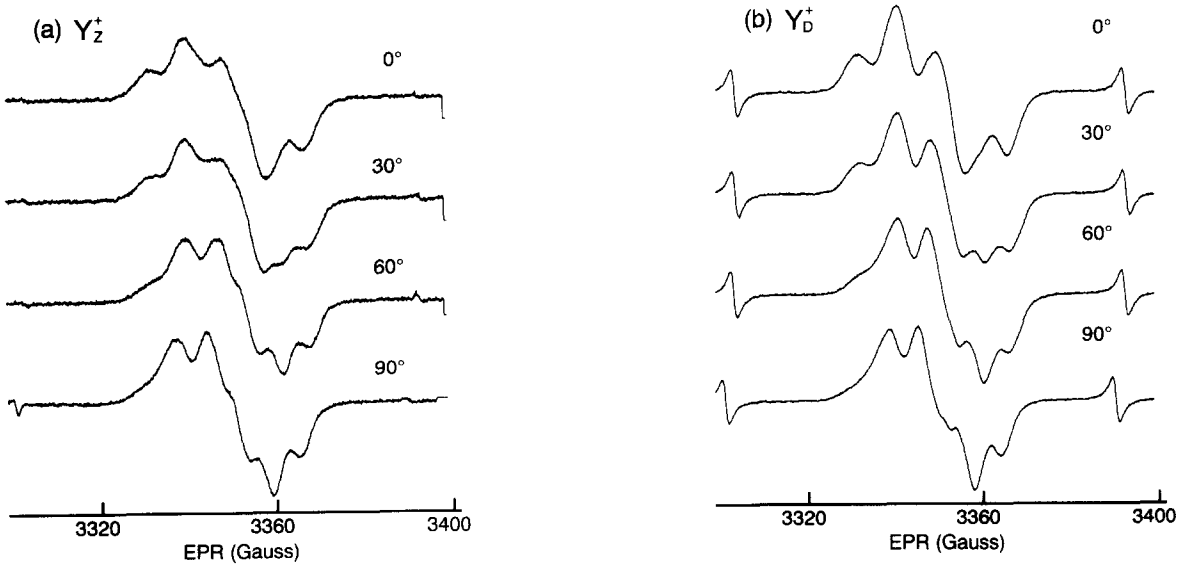

Fig. 4. EPR spectra of Y_Z^+(a) and Y_D^+(b) obtained in oriented PS II membranes at different directions of the external magnetic field with respect to the membrane normal. Mn(II) in MgO was used as a reference for field position. EPR conditions are same as in Fig. 1 except for the temperature of 100 K.

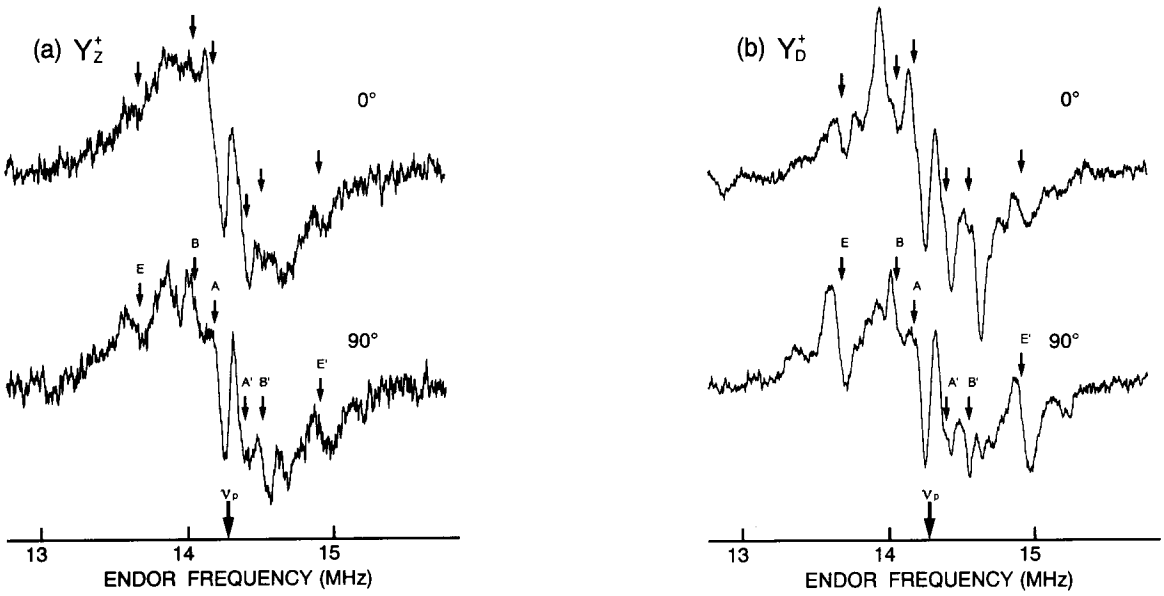

Fig. 5. ENDOR spectra of Y_Z^+ (a) and Y_D^+ (b) in the frequency range of 3 MHz obtained in oriented PS II membranes at two different directions of the external magnetic field vector with respect to the membrane normal. ENDOR conditions are the same as in Fig. 2.

Fig. 5 shows the ENDOR spectra observed within 3 MHz range in the oriented membranes at 10 K. Both species have similar orientation dependence, though it is remarkable that the resolution of the spectra for the field direction along the membrane normal (0°) is much worse for Y_Z^+ than that for Y_D^+. AA', BB' and EE' peaks show the same orientation dependence in both radicals. Furthermore the other peaks corresponding to the CC', DD' and FF' peaks corresponding to the powder patterns in Fig. 2a and b seem to show the same orientation dependence. These features suggest that the protons surrounding both radicals also have similar configurations with some minor modifications in distances from each tyrosine molecule. These modifications may have caused the lower resolution of the spectra for the field direction 0° in Y_Z^+.

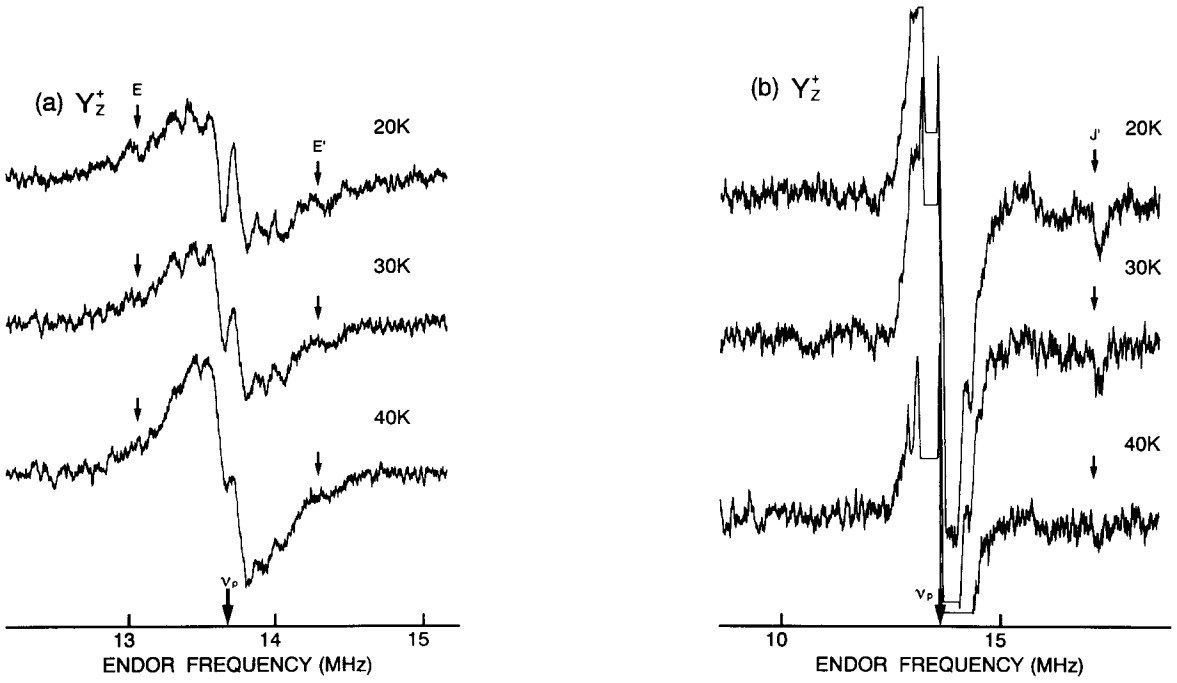

Fig. 6. Temperature dependence of ENDOR spectra of Y_Z^+ in the ranges of 3 MHz (a) and 10 MHz (b). ENDOR conditions of (a) and (b) are the same as in Fig. 2 and Fig. 3, respectively.

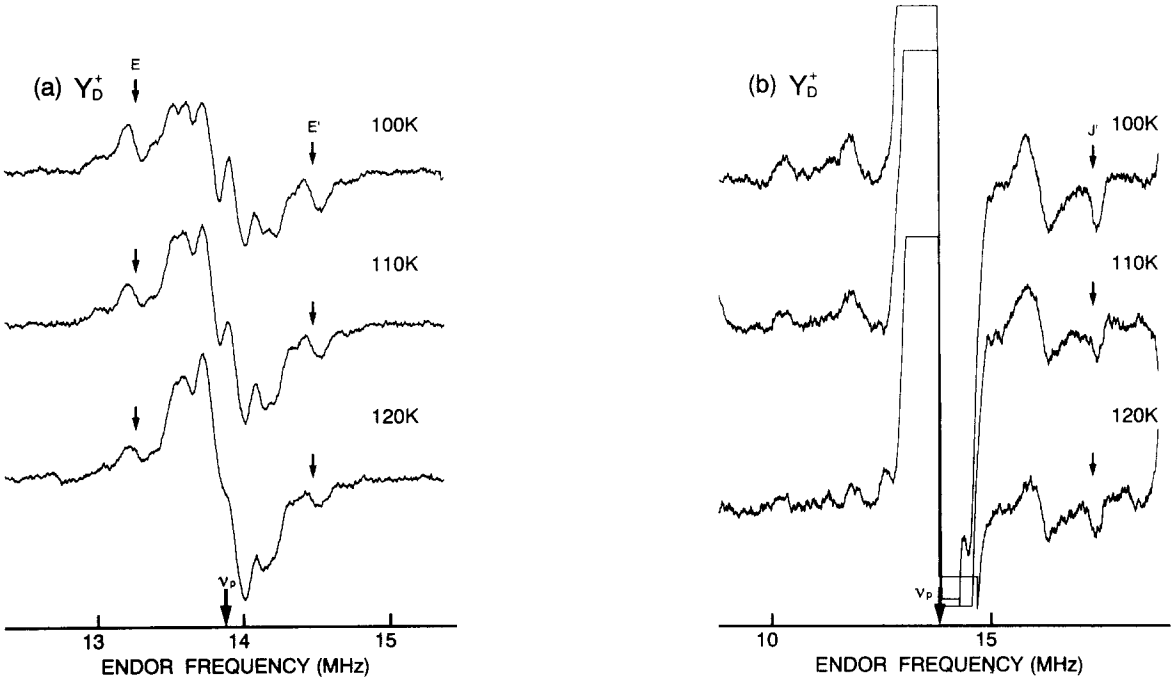

Fig. 7. Temperature dependence of ENDOR spectra of Y_D^+ in the ranges of 3 MHz (a) and 10 MHz (b). ENDOR conditions are the same as in Fig. 6.

Fig. 6a shows the temperature variation of matrix ENDOR spectra within 3 MHz range for Y_Z^+. Above 30 K, the intensity of the EE′ peaks decreases (Fig. 6a). Corresponding to this decrease, the intensity of the J′ peak in Fig. 6b also decreases. Other peaks are not visible because of low S/N ratio and decrease of their intensity due to broadening. Fig. 7a and b show the temperature variation of matrix ENDOR spectra of Y_D^+ in 3 MHz range and in 10 MHz range respectively. Above 110 K, the similar temperature variations in EE′ and JJ′ peaks were observed for Y_D^+. As the temperature increases, the resolution of ENDOR spectra for both radical species tends to decrease. Though both radicals have similar lineshapes of ENDOR spectra at the low temperature of 10 K, their temperature variations are different, which we may attribute to the difference in molecular dynamics of the surrounding protons.

4. Discussion

Both Y_Z^+ and Y_D^+ radicals have similar molecular orientation, with the C-O bond being directed along the membrane normal as judged from EPR spectra in the oriented membranes (Fig. 4a and b). The ENDOR spectra observed for both radicals suggest similar orientational configurations of the surrounding protons. Considering the orientational dependence of the ENDOR spectra in our previous report [28], we have shown the radius vectors to the five proton positions contributing to AA′ BB′ CC′ EE′ and FF′ lines to be directed approximately parallel to the membrane plane. Of the ENDOR lines produced by these five kinds of proton, the EE′ peaks show the most remarkable temperature variation. We tentatively ascribe the decrease in their intensity to the line broadening caused by the hindered vibration of the corresponding protons. The

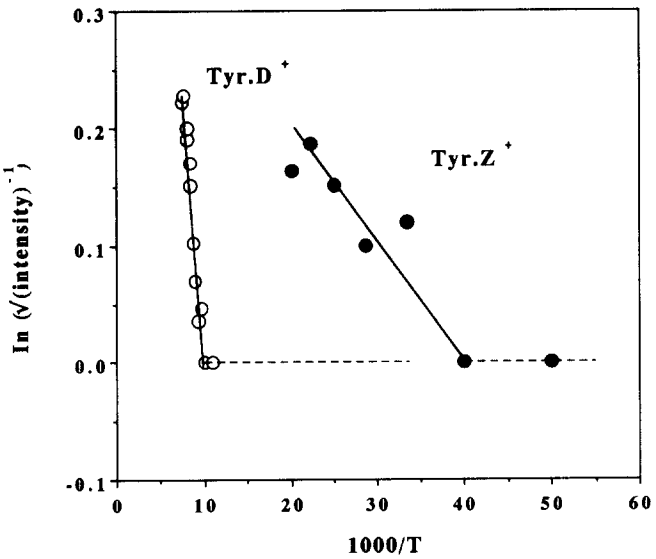

Fig. 8. Inverse square root of the relative intensity of the peaks EE′ of ENDOR spectra of Y_Z^+ and Y_D^+ shown by open and closed circles, respectively. The activation energies are 86±20 J/mol between 25 K and 50 K for Y_Z^+ and 810±200 J/mol between 110 K and 130 K for Y_D^+.

other factors, such as change of the ENDOR enhancement through spin lattice relaxation caused by local molecular motions, might be also taken into consideration, though their analysis represents a complicated problem [29]. On the other hand, the effect of the line broadening due to the difference in separations given by Eq. (1) can be easily estimated.

In our model for the line broadening of the ENDOR spectra, a proton is assumed to take a fixed position at low temperatures. With increasing temperature some modes of hindered vibrations will be excited and the proton will occupy several positions. Since the electron nuclear dipole interactions in these positions are slightly different, the corresponding ENDOR lines will be broadened and show smaller intensity. Assuming that the peak height of the first derivative ENDOR spectrum is inversely proportional to the square of the line width, we can estimate the activation energy for the proton to change its position.

As shown above the effect of the motional broadening is most pronounced for the EE′ proton. Fig. 8 shows the Arrhenius plot of the line width estimated by the inverse square root of the intensity of the EE′ peaks for both tyrosine radicals. The intensities were normalized by the integrated spectral intensity within 3 MHz range. Using the expression;

$$\delta\nu = \delta\nu_0 \exp(-E_A/kT) \quad (2)$$

where $\delta\nu$ is the estimated line width, E_A is the activation energy and k is the Boltzmann constant, one can evaluate the activation energy for broadening of EE′ peaks from Eq. (2) as;

86 ± 20 J/mol for Y_Z^+ between 25 K and 50 K,

and

810 ± 200 J/mol for Y_D^+ between 110 K and 130 K.

The derived values show some relative difference in motional characteristics between both radicals. Y_Z^+ has a lower activation energy corresponding to the lower characteristic temperature for its line broadening. $\delta\nu_0$ was estimated by spectrum simulations to be about 50 kHz, corresponding to the amplitude of vibration of about 0.2 Å for both tyrosine radicals.

Though the amplitude of the motions is small, it suggests the presence of some mobile amino groups around these radical species. The difference in the activation energies can be ascribed to the difference in flexibility of environment of these radicals. These results suggest that, according to the proton rocking model [12,14] electron transfer in Y_Z is more efficient than that in Y_Z^+.

The lower activation energy in Y_Z^+ is very reasonable, when we consider that Y_Z^+ is unstable at physiological temperatures, while Y_D^+ is stable whether it is in oxygen-evolving PS II or in Tris-treated PS II. At physiological temperatures there should be much more freedom for motions which activate Y_Z^+ in D1 proteins. Y_Z is considered to be in a relatively hydrophilic environment [19] and may be more easily affected by charges on the membrane surface [13] and by structural modification via phase change of lipid or depletion of some proteins [10–12].

Marcus and Sutin [30] reviewed various kinds of electron transfer reaction and discussed a steric effect on an electron transfer rate. Molecular vibration observed in EE′ peaks might induce vibrations due to hydrogen bonding protons resulting in decrease of the corresponding ENDOR lines (JJ′ in Fig. 6b). The difference in temperature ranges of excitation of the hindered vibrations observed in EE′ peaks between Y_Z^+ and Y_D^+ may be ascribed to the relative hydrophilic affinities of the surrounding amino acids.

As mentioned above, the temperature variations of the ENDOR spectra of Y_Z^+ and Y_D^+ can be explained also by the changes of the enhancement factors due to changes in spin-lattice relaxation rates. Since the spin-lattice relaxation also reflects the mobility in the environment of the radicals, this explanation will lead to the qualitatively same conclusion about greater mobility of the surroundings of the Y_Z^+ as compared with that of Y_D^+.

The low-temperature characteristics observed by proton matrix ENDOR reflect the frozen structure of a part of the microenvironment of the two tyrosine radicals at the illumination temperature of 253 K. The potential barriers for molecular motions of protons surrounding Y_Z^+ and Y_D^+ are considered to have relevance to the electron transfer functions above this temperature.

References

[1] Debus, R.J., Barry, B.A., Sithole, I., Babcock, G.T. and McIntosh, L. (1988) Biochemistry 27, 9071–9074.
[2] Metz, J.G., Nixon, P.J., Rögner, M., Brudvig, G.W. and Diner, B.A. (1989) Biochemistry 28, 6960–6969.
[3] Debus, R.J., Barry, B.A., Babcock, G.T. and McIntosh, L. (1988) Proc. Natl. Acad. Sci. USA 85, 427–430.
[4] Vermaas, W.F.J., Rutherford, A.W. and Hansson, O. Proc. Natl. Acad. Sci. USA 85, 8477–8481.
[5] Inui, T., Kawamori, A., Kuroda, G., Ono, T., and Inoue, Y. (1989) Biochim. Biophys. Acta 973, 147–152.
[6] Styring, S and Rutherford A.W. (1987) Biochemistry 26, 2401–2405.
[7] Babcock, G.T. and Sauer, K. (1975) Biochim. Biophys. Acta 376, 329–344.
[8] Warden, J.T., Blankenship, R.E. and Sauer, K. (1976) Biochim. Biophys. Acta 423, 462–478.
[9] Babcock, G.T. and Sauer, K. (1975) Biochim. Biophys. Acta 276, 315–328.
[10] Haveman, J. and Mathis, P. (1976) Biochim. Biophys. Acta 440, 346–355.

[11] Reinman, S. and Mathis, P. (1981) Biochim. Biophys. Acta 635, 249–258.
[12] Eckert, H.-J. and Renger, G. (1988) FEBS Lett. 236, 425–431.
[13] Conjeaud, H. and Mathis, P. (1986) Biophys. J. 49, 1215–1221.
[14] Babcock, G.T., Barry, B.A., Debus, R.J., Hoganson, C. W., Atamian, M., McIntosh, L., Sithole, I. and Yocum, C.F. (1989) Biochemistry 28, 9557–9565.
[15] Barry, B.A. and Babcock, G.T. (1987) Proc. Natl. Acad. Sci. USA 84, 7099–7103.
[16] Kodera, Y., Takura, K., Mino, H. and Kawamori, A. (1992) in Research in Photosynthesis (Murata, N., ed.), Vol. II, pp. 57–60, Kluwer, Dordrecht.
[17] Barry, B.A., El-Deeb, M.K., Sandusky, P.O. and Babcock, G.T. (1990) J. Biol. Chem. 265, 20139–20143.
[18] Evelo, R.G., Hoff, A.J., Dikanov, S.A. and Tyryshkin, A.M. (1989) Chem. Phys. Lett. 161, 479–484.
[19] Svensson, B., Vass, I. and Styring, S. (1991) Z. Naturforsch. 46c, 765–776.
[20] Brustolon, M. (1989) Advanced EPR (Hoff, A.J. ed.), pp. 593–614 Elsevier Science Publishers B.V., The Netherlands. 14.
[21] Kurreck, H., Bock, M., Bretz, N., Elsner, M., Klaus, H., Lubitz, W., Muller, F., Geissler, J. and Kroneck, P.M.H. (1984) J. Am. Chem. Soc. 106, 737–746.
[22] Mino, H., Kodera, Y. and Kawamori, A. (1992) in Research in Photosynthesis (Murata, N., ed.), Vol. II, pp. 61–64, Kluwer, Dordrecht.
[23] Styring, S. and Rutherford, A.W. (1988) Biochim. Biophys. Acta 933, 378–387.
[24] Kuwabara, T. and Murata, N. (1982) Plant Cell Physiol. 23, 533–539.
[25] Rutherford, A.W. (1985) Biochim. Biophys. Acta 807, 189–201.
[26] Kawamori, A., Inui, T. Ono, T. and Inoue. Y. (1989) FEBS Lett. 254, 219–224.
[27] Miller, A.-F. De Paula, J.C. and Brudvig, G.W. (1987) Photosynth. Res. 12, 205–218.
[28] Mino, H., Satoh, J., Kawamori, A., Toriyama, K. and Zimmermann, J.-L. (1993) Biochim. Biophys. Acta 1144, 426–433.
[29] Kevan, L. and Narayana, P.A. (1979) Multiple Electron Resonance Spectroscopy (Dorio, M.M. and Freed J.H., eds.), pp. 229–259, Plenum Press, New York.
[30] Marcus, R.A. and Sutin, N. (1985) Biochim. Biophys. Acta 811, 265–322.